Comparative Study of the Oxidation of Fluorene and 9,9-Disubstituted Fluorenes and Their Related 2,7′-Dimers and Trimer

Philippe Hapiot, Corinne Lagrost, Fabien Le Floch, Eugène Raoult, and Joëlle Rault-Berthelot*

Laboratoire d'Electrochimie Moléculaire et Macromoléculaire, UMR CNRS 6510: Synthèse et Electrosynthèse Organiques, Institut de Chimie de Rennes, Campus de Beaulieu, Avenue du Général Leclerc, 35042 Rennes, France

Received September 23, 2004. Revised Manuscript Received February 4, 2005

Electroactive polyfluorene films were obtained by anodic coupling of fluorene and a series of 9,9-disubstituted fluorenes and their related 2,7′-dimers and trimer. The polymerization mechanism is discussed in light of cyclic voltammetry investigations in organic media using the classical millimetric electrode and ultramicroelectrodes, DFT theoretical calculations, and laser flash photolysis experiments. The first step of electropolymerization involves the formation of the carbon−carbon bond through the coupling between two fluorene radical cations. However, the radical cation of the produced dimer is not reactive enough to repeat the coupling reaction as in the classical electropolymerization mechanism. To continue the polymerization, formation of a higher oxidation state is required. This behavior is supported by theoretical expectations.

Introduction

The polyfluorene structure (Scheme 1) can be regarded as a substituted polyphenylene with a pair of phenyl rings locked into planar arrangement by the presence of the C_9 atom. In the polymer, successive fluorene units are linked through C_2 and C_7 atoms. Solubilizing substituents can be attached to the C_9 position without introducing torsional strain on the fluorene group. The derived fluorene-based materials are highly fluorescent and are used as an active material in LED (light electroluminescent diode) devices.[1] Numerous examples of such LEDs (see, for example, the devices based on poly(9,9-dihexylfluorene)[2a] or poly(9,9-dioctylfluorene)[2b] as emitting layers) have been described in the literature as blue-light-emitting diodes at room temperature with interesting features.

Several chemical and electrochemical methods have been reported for preparing polyfluorenes: oxidative polymerization of 9-alkyl- or 9,9-dialkylfluorenes in the presence of $FeCl_3$,[3a] transition-metal-catalyzed reactions (Yamamoto's[3b] or Suzuki's[3c] coupling reactions), electropolymerization on electrodes,[4] .... Electrochemical polymerization can be achieved

Scheme 1. Polyfluorene Structure

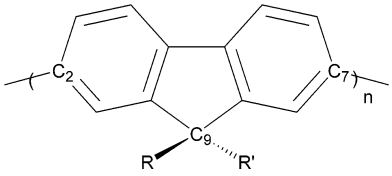

by either cathodic[4a] or anodic processes,[4b−d] the last one being the most described method. Despite the large number of publications dealing with anodically synthesized polyfluorenes, there are very few investigations concerning the fluorene polymerization mechanisms,[5] due to the lack of data concerning the reactive intermediates. It is generally assumed that the reaction follows the same mechanistic scheme as that proposed for other conducting polymers such as polypyrrole or polythiophene.[6] For these materials, the polymerization involves a series of consecutive electrochemical and chemical steps, namely, heterogeneous and homogeneous electron-transfer processes, carbon−carbon bond formations, and deprotonations.[6,7] The nature of the first key steps has been elucidated for thiophene and pyrrole series.[6b,c,7] In both

* To whom correspondence should be addressed. E-mail: Joelle.Rault@univ-rennes1.fr.

(1) Rault-Berthelot, J. *Res. Trends Res.* **2004**, *10*, 265 and references therein.

(2) (a) Ohmori, Y.; Uchida, M.; Muro, K.; Yoshino, K. *Jpn. J. Appl. Phys.* **1991**, *30*, L1941. (b) Grell, M.; Bradley, D. D. C.; Ungar, G.; Hill, J.; Whitehead, K. S. *Macromolecules* **1999**, *32*, 5810.

(3) (a) Fukuda, M.; Sawaka, K.; Yoshino, K. *J. Polym. Sci., Polym. Chem. Ed.* **1993**, *31*, 2465. (b) Yamamoto, T. *Prog. Polym. Sci.* **1992**, *17*, 1153. (c) Miyaura, N.; Yanagi, T.; Suzuki, A. *Synth. Commun.* **1981**, *11*, 513.

(4) (a) Schiavon, G.; Zotti, G.; Bontempelli, G. *J. Electroanal. Chem.* **1985**, *186*, 191. (b) Rault-Berthelot, J.; Simonet, J. *J. Electroanal. Chem.* **1985**, *182*, 187. (c) Waltman, J.; Bargon, J. *J. Electroanal. Chem.* **1985**, *182*, 187. (d) Rault-Berthelot, J. *Recent Res. Dev. Macromol. Res.* **1998**, *3*, 425.

(5) (a) A recent paper reports on a comparative study of polyfluorene growth in CH_2Cl_2 and CH_3CN in the presence of BF_4^- anions.[5b] (b) Sharma, H. S. Park, S.-M. *J. Electrochem. Soc.* **2004**, *151*, E61−E68.

(6) (a) Genies, E. M.; Bidan, G.; Diaz, A. F. *J. Electroanal. Chem.* **1983**, *149*, 101. (b) Andrieux, C. P.; Audebert, P.; Hapiot, P.; Savéant, J.-M. *J. Am. Chem. Soc.* **1990**, *112*, 2439. (c) Andrieux, C. P.; Audebert, P.; Hapiot, P.; Savéant, J.-M. *J. Phys. Chem.* **1991**, *95*, 10158. (d) *Handbook of Organic Conductive Molecules and Polymers*; Nalva, H. S., Ed.; John Wiley and Sons: New York, 1997; Vol 2.

(7) (a) Zotti, G.; Schiavon, G.; Berlin, A.; Pagani, G. *Chem. Mater.* **1993**, *5*, 430. (b) Zhou, M.; Heinze, J. *J. Phys. Chem. B* **1999**, *103*, 8443. (c) Zhou, M.; Heinze, J. *J. Phys. Chem. B* **1999**, *103*, 8451. (d) Hapiot, P.; Lagrost, C.; Aeiyach, S.; Jouini, M.; Lacroix, J.-C. *J. Phys. Chem. B* **2002**, *106*, 3622. (e) Lacroix, J.-C.; Maurel, F.; Lacaze, P.-C. *J. Am. Chem. Soc.* **2001**, *123*, 1989.

10.1021/cm048331o CCC: $30.25
Published on Web 03/23/2005

Scheme 2. Studied Structures

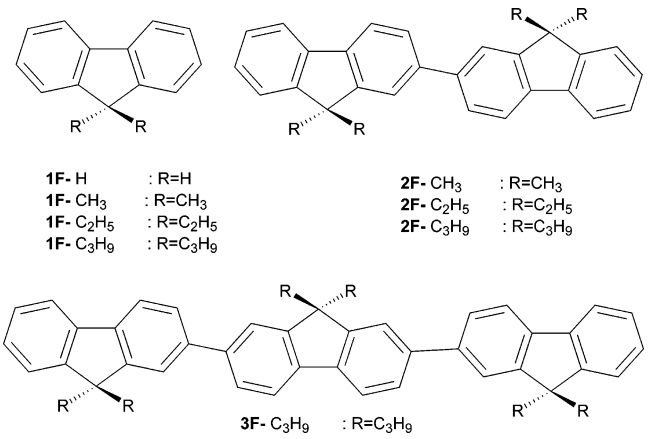

cases the carbon−carbon bond formation proceeds through the coupling of two cation radicals followed by the deprotonation of the resulting dihydrodimer dication.[7] The importance of the deprotonation reactions on the quality of the polymer has been clearly demonstrated in the case of the electropolymerization of pyrrole. The presence of water or acidic traces can create considerable transitions between polypyrrole variants.[8] Deprotonation steps are intrinsically slow because they involve C−H bonds breaking in a carbon acid.[9] However, it is unclear whether this mechanism remains valid for polyfluorenes as little is known about the reactivities of fluorene and oligofluorene radical cations. In this work, the oxidative coupling of various 9,9-disubstituted fluorenes 1F−R and their related 2,7′-dimers 2F−R and trimer 3F−C_3H_7 (Scheme 2) was investigated.

The properties of the corresponding radical cations in organic solvents were examined in relation to electroactive film formation. Mechanistic and kinetic investigations were performed to gain a better understanding of the parameters determining the quality of the film. For the purpose of comparison, the oxidation of the unsubstituted fluorene 1F−H was also reexamined in the same experimental conditions. In light of these observations, we tried to determine more specifically the nature of the species involved in the oxidation process of 1F−H and 1F−R and to compare the anodic behavior of 1F−H and 1F−R with that of 2F−R and 3F−C_3H_7.

Experimental Section

Chemicals. Acetonitrile with less than 5‰ water (reference SDS 00610S21) and dichloromethane with less than 100 ppm water (reference SDS 02910E21) were used without purification. Tetrabutylammonium hexafluorophosphate from Fluka (electrochemical grade) was used without purification. Fluorene 1F−H is a commercially available product and was used without additional purification. 1F−R and 2F−R were synthesized according to the literature,[10] and 3F−C_3H_7 was synthesized by an analogous route along a Kumada reaction.

Data for 1F−CH_3. White solid. Yield: 96%. Mp: 92−93 °C. ^{1}H NMR ($CDCl_3$): δ/ppm 1.41 (s, 6H, CH_3), 7.24 (m, 4H, CH_{Ar}), 7.36 (d, 2H, CH_{Ar}, J = 7.00 Hz), 7.65 (d, 2H, CH_{Ar}, J = 6.25 Hz). ^{13}C NMR ($CDCl_3$): δ/ppm 21.28 (CH_3), 55.18 ($C_{q(9)}$), 120.11 ($CH_{Ar(4,5)}$), 122.72 ($CH_{Ar(2,7)}$), 127.06 ($CH_{Ar(1,8)}$), 127.35 ($CH_{Ar(3,6)}$), 139.31 ($C_{q(10,12)}$), 153.71 ($C_{q(11,13)}$). HRMS: m/z calcd for $C_{15}H_{14}$ 194.10955, found 194.10622. Anal. Found: C, 91.70 (calcd 92.74); H, 7.32 (calcd 7.26).

Data for 1F−C_2H_5. White solid. Yield: 98%. Mp: 31 °C. ^{1}H NMR ($CDCl_3$): δ/ppm 0.32 (t, 6H, CH_3, J = 7.58 Hz), 2.03 (q, 4H, CH_2, J = 7.58 Hz), 7.32 (m, 6H, CH_{Ar}), 7.71 (m, 2H, CH_{Ar}). ^{13}C NMR ($CDCl_3$): δ/ppm 8.61 (CH_3), 32.87 (CH_2), 56.17 ($C_{q(9)}$), 119.87 ($CH_{Ar(4,5)}$), 123.04 ($CH_{Ar(2,7)}$), 126.89 ($CH_{Ar(1,8)}$), 127.13 ($CH_{Ar(3,6)}$), 141.66 ($Cq_{(10,12)}$), 149.97 ($Cq_{(11,13)}$). HRMS: m/z calcd for $C_{17}H_{18}$ 222.14085, found 222.14000.

Data for 1F−C_3H_7. Yellow solid. Yield: 96%. Mp: 29 °C. ^{1}H NMR ($CDCl_3$): δ/ppm 0.32 (t, 6H, CH_3, J = 7.58 Hz), 2.03 (q, 4H, CH_2, J = 7.58 Hz), 7.32 (m, 6H, CH_{Ar}), 7.71 (m, 2H, CH_{Ar}). ^{13}C NMR ($CDCl_3$): δ/ppm 14.55 (CH_3), 17.31 (CH_2), 42.92(CH_2), 55.34 ($C_{q(9)}$), 119.77 ($CH_{Ar(4,5)}$), 122,98 ($CH_{Ar(2,7)}$), 126.85 ($CH_{Ar(1,8)}$), 127.13 ($CH_{Ar(3,6)}$), 141.22 ($C_{q(10,12)}$), 150.80 ($C_{q(11,13)}$). HRMS: m/z calcd for $C_{19}H_{22}$ 250.17215, found 250.17230. Anal. Found: C, 91.41 (calcd 91.14); H, 8.78 (calcd 8.86).

Data for 2F−CH_3. White solid. Yield: 28%. Mp: 217 °C. ^{1}H NMR ($CDCl_3$): δ/ppm 1.59 (ms 12H, CH_2), 7.35 (m, 4H, CH_{Ar}), 7.49 (m, 2H, CH_{Ar}), 7.61−7.91 (m, 8H, CH_{Ar}). ^{13}C NMR ($CDCl_3$): δ/ppm 27.57 (CH_2), 47.11 (C_q), 120.41, 121.53, 122.75, 126.41, 127.16, 127.35, 138.49, 139.02, 140.93, 154.01, 154.38, 120.18. HRMS: m/z calc for $C_{30}H_{26}$ 386.20345, found 386.20205. Anal. Found: C, 89.48 (calcd 93.22); H, 6.60 (calcd 6.78).

Data for 2F−C_2H_5. White solid. Yield: 30%. Mp: 198 °C. ^{1}H NMR ($CDCl_3$): δ/ppm 0.41 (t, 12H, CH_3, ^3J = 4.91 Hz), 2.13 (q, 8H, CH_2), 7.35 (m, 6H, CH_{Ar}), 7.66 (m, 2H, CH_{Ar}), 7.76 (m, 2H, CH_{Ar}). ^{13}C NMR ($CDCl_3$): δ/ppm 8.74 (CH_2), 32.94 (CH_2), 56.34 (C_q), 119.80, 119.96, 121.53, 123.04, 126.22, 126.97, 127.09, 140.67, 140.80, 141.35, 150.25, 150. HRMS: m/z calcd for $C_{34}H_{34}$ 442.26605, found 442.26357.

Data for 2F−C_3H_7. Pale yellow solid. Yield: 34%. Mp: 157 °C. ^{1}H NMR ($CDCl_3$): δ/ppm 0.72 (m, 20H, CH_3, CH_2), 2.05 (m, 8H, CH_2), 7.36 (m, 6H, CH_{Ar}), 7.60 (s, 2H, CH_{Ar}), 7.65 (d, 2H, ^3J = 7.86 Hz), 7.78 (m, 4H, CH_{Ar}). ^{13}C NMR ($CDCl_3$): δ/ppm 13.85 (CH_2), 42.95 (CH_2), 55.53 (CH_2), 119.84, 120.01, 121.48, 123.05, 126.20, 126.94, 127.12, 140.48, 140.61, 140.92, 151.12, 151.56. HRMS: m/z calcd for $C_{38}H_{42}$ 498.32865, found 498.32722. Anal. Found: C, 88.57 (calcd 91.51); H, 8.30 (calcd 8.49).

Data for 3F−C_3H_7. Yellow solid. Yield: 17%. Degradation at 150 °C. ^{1}H NMR ($CDCl_3$): δ/ ppm 0.54−0.97 (m, 30H, CH_3, CH_2), 1.88−2.28 (m, 12H, CH_2), 7.26−7.52 (m, 6H, CH_{Ar}), 7.58−7.71 (m, 8H, CH_{Ar}), 7.71−7.84 (m, 6H, CH_{Ar}). ^{13}C NMR ($CDCl_3$): δ/ppm 14.56, 17.35, 42.85, 55.52, 119.86, 120.03, 120.09, 121.48, 121.56, 123.07, 126.21, 126.31, 126.95, 124.14, 140.09, 140.28, 140.44, 140.60, 140.90, 151.14, 151.60, 151.89. MS (Zabspec TOF): m/z calcd for $C_{57}H_{62}$ 746.48515, found 746.4849. Anal. Found: C, 87.32 (calcd 91.64); H, 8.36 (calcd 8.18).

Electrochemical Setup and Procedures. All electrochemical experiments were performed using a three-electrode cell setup. The working electrode was a Pt disk electrode (1 mm diameter for low-scan-rate experiments or a 10 μm diameter ultramicroelectrode for fast-scan-rate experiments), the counter electrode was a vitreous carbon rod, and the reference electrode was a silver wire in a 0.1 mol·L^{-1} $AgNO_3$ solution in CH_3CN. The working electrode was carefully polished before each voltammetry experiment with 1 μm diamond paste and ultrasonically rinsed in absolute ethanol. Electrolyte solutions were thoroughly purged and kept under a dry

(8) Zhou, M.; Pagels, M.; Geschke, B.; Heinze, J. *J. Phys. Chem. B* **2002**, *106*, 10065 and references therein.
(9) Gamby, J.; Hapiot, P.; Savéant, J.-M. *J. Am. Chem. Soc.* **2002**, *124*, 8798.
(10) (a) Tamao, K.; Kodama, S.; Nakajima, I.; Kumada, M.; Minato, A.; Suzuki, K. *Tetrahedron* **1982**, *38*, 3347. (b) Tamao, K.; Kiso, Y.; Sumitani, K.; Kumada, M. *J. Am. Chem. Soc.* **1972**, *94*, 9268. (c) Murphy, W. S.; Hauser, C. R. *J. Org. Chem.* **1966**, *31*, 85.

argon flow during each run. Experiments were performed at room temperature (20 ± 2 °C). Ferrocene was added at the end of a series of experiments as an internal standard. All potentials are referenced to the ferrocene/ferrocenium (F_c/F_c^+) couple. Because of the possible sensitivity of the polymerization reaction to the presence of water, activated Al_2O_3 was added to the electrolytic solution to remove excess moisture. The residual water content in the medium was checked before addition of the monomer during cyclic voltammetry at 100 mV·s^{-1} between −2.0 and +2.0 V, using a platinum electrode of diameter 1 mm. The current must be less than 1 μA at −2.0 and +2.0 V, which corresponds to a concentration of water lower than 30 ppm. For low- and moderate-scan-rate cyclic voltammetry (up to 500 V·s^{-1}), electrochemical instrumentation consisted of a Tacussel GSTP4 programmer and a home-built potentiostat equipped with a positive-feedback compensation device.[11] The voltammograms were recorded with a 310 Nicolet oscilloscope. For high-scan-rate voltammetry using an ultramicroelectrode, the signal generator was an Agilent 33250A, and the data were acquired with an Agilent Infiniium oscilloscope (500 MHz, 1 Gsample/s).

Numerical simulations of the voltammograms were performed with the BAS DigiSim simulator 3.03, using the default numerical options with the assumption of planar diffusion and a Butler−Volmer law for the electron transfer. The charge-transfer coefficient, α, was taken as 0.5, and the diffusion coefficients were taken equal for all species ($D = 10^{-5}$ cm^2·s^{-1}).

Laser Flash Photolysis Experiments. The equipment and experimental procedures have been thoroughly described in previous papers.[7d] Irradiations were performed with a Compex 100 (Lambda Physik) excimer laser (100−150 mJ/20−50 ns) filled with a XeCl mixture ($\lambda = 308$ nm). The detection system consisted of a 150 W xenon lamp, a 0.5 cm optical path length irradiation cell, an ARC SP 150 spectrograph (Acton Research Corp., Acto, MA), and an intensified diode array system (PG200 pulsed generator, ST-121 controller, and IRY-700 S/RB detector from Princeton Instruments, Inc., Princeton, NJ). For the acquisition, the pulse width was set to 100 ns, and the delay after the laser pulse was adjusted to be as short as possible to avoid the observation of a laser flash or fluorescence from the fluorenes. When required, spectra were averaged to improve the signal-to-noise ratio.

Theoretical Modeling. The calculations were performed using the Gaussian 98 package[12] for density functionals. Gas-phase geometries and electronic energies were calculated by full optimization without imposed symmetry of the conformations using the B3LYP[13] density functional with the 6-31G* basis set[14] starting from preliminary optimizations performed with semiempirical methods. Because of the difficulty to run frequency calculations with the large investigated molecules, the quality of the obtained minima was checked by restarting the optimizations from other conformations which led to the same optimized geometries. In the open shell B3LYP calculations, the spin contamination remains low ($s^2 < 0.755$) for radical cations but slightly increases for the trication radical trimer ($s^2 = 1.04$).

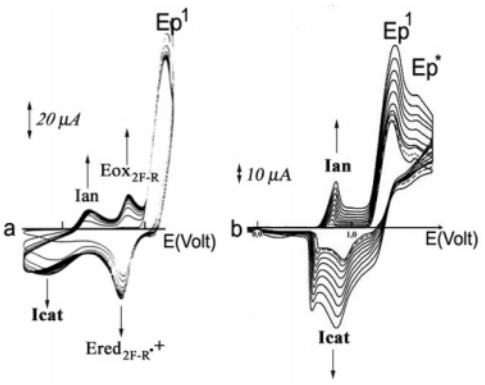

Figure 1. Cyclic voltammetry in dry CH_2Cl_2 + 0.2 mol·L^{-1} Bu_4NPF_6 in the presence of 1F−CH_3 at a concentration of 10^{-2} mol·L^{-1} on a 1 mm diameter platinum disk: (a) Multiple cycles between 0.0 and 1.4 V at a scan rate of 1 V·s^{-1}, (b) multiple cycles between 0.0 and 2.0 V at a scan rate of 0.1 V·s^{-1}.

Results and Discussion

Although electropolymerization of 1F−H is very efficient in acetonitrile,[4b] oxidation of 9,9-disubstituted fluorenes 1F−R and corresponding oligomers *n*F−R was principally studied in CH_2Cl_2 + Bu_4NPF_6, which offers a good solubility even for the longest investigated oligomers (at concentrations of several 10^{-3} mol·L^{-1}). For comparison, some additional experiments were also performed in CH_3CN. Oxidative polymerization was always observed in CH_2Cl_2 + Bu_4NPF_6 (see below), but as expected, the polymerization yield was found to be sensitive to the choices of solvent and supporting electrolyte, and more detailed investigations concerning the effects and optimization of the experimental conditions will be the subject of a further publication.

Oxidation of 9,9-Disubstituted 1F−R and Unsubstituted 1F−H Fluorenes. In CH_2Cl_2, the oxidations of the different 1F−R and of 1F−H fluorenes investigated by cyclic voltammetry exhibit similar general patterns whatever the length of the substituent R. During the first cycle and at a low scan rate (see Figure 1b at 0.1 V·s^{-1} in the case of 1F−CH_3), a main irreversible oxidation peak (with a peak potential E_p^1 at about 1.32−1.33 V) followed by a second less intense peak located at E_p* (around 1.6 V for all compounds) is visible. The main remarkable feature is that the polymerization (or oligomerization) only occurs when the inversion potential is chosen to be more positive than E_p* (compare parts a and b of Figure 1). In such a case, the appearance and the regular increase, during the multiple cycles, of a new reversible wave labeled I_{an}/I_{cat} between 0.5 and 1.5 V is characteristic of the formation of an electroactive and conductive layer onto the electrode. On the contrary, when the cycle is limited to the first oxidation process E_p^1 (see Figure 1a), one can observe during the reverse cycle, at a high scan rate, the appearance of two systems. By comparison with an authentic sample, the more positive peak

(11) Garreau, D.; Savéant, J.-M. *J. Electroanal. Chem.* **1972**, *35*, 309.
(12) Frisch, M. J.; Trucks, G. W.; Schlegel, H. B.; Scuseria, G. E.; Robb, M. A.; Cheeseman, J. R.; Montgomery, J. A., Jr.; Vreven, T.; Kudin, K. N.; Burant, J. C.; Millam, J. M.; Iyengar, S. S.; Tomasi, J.; Barone, V.; Mennucci, B.; Cossi, M.; Scalmani, G.; Rega, N.; Petersson, G. A.; Nakatsuji, H.; Hada, M.; Ehara, M.; Toyota, K.; Fukuda, R.; Hasegawa, J.; Ishida, M.; Nakajima, T.; Honda, Y.; Kitao, O.; Nakai, H.; Klene, M.; Li, X.; Knox, J. E.; Hratchian, H. P.; Cross, J. B.; Adamo, C.; Jaramillo, J.; Gomperts, R.; Stratmann, R. E.; Yazyev, O.; Austin, A. J.; Cammi, R.; Pomelli, C.; Ochterski, J. W.; Ayala, P. Y.; Morokuma, K.; Voth, G. A.; Salvador, P.; Dannenberg, J. J.; Zakrzewski, V. G.; Dapprich, S.; Daniels, A. D.; Strain, M. C.; Farkas, O.; Malick, D. K.; Rabuck, A. D.; Raghavachari, K.; Foresman, J. B.; Ortiz, J. V.; Cui, Q.; Baboul, A. G.; Clifford, S.; Cioslowski, J.; Stefanov, B. B.; Liu, G.; Liashenko, A.; Piskorz, P.; Komaromi, I.; Martin, R. L.; Fox, D. J.; Keith, T.; Al-Laham, M. A.; Peng, C. Y.; Nanayakkara, A.; Challacombe, M.; Gill, P. M. W.; Johnson, B.; Chen, W.; Wong, M. W.; Gonzalez, C.; Pople, J. A. *Gaussian 03*, revision B.04; Gaussian, Inc.: Pittsburgh, PA, 2003.
(13) Becke, A. D. *J. Chem. Phys.* **1993**, *98*, 5648.
(14) Hariharan, P. C.; Pople, J. A. *Chem. Phys. Lett.* **1972**, *16*, 217.

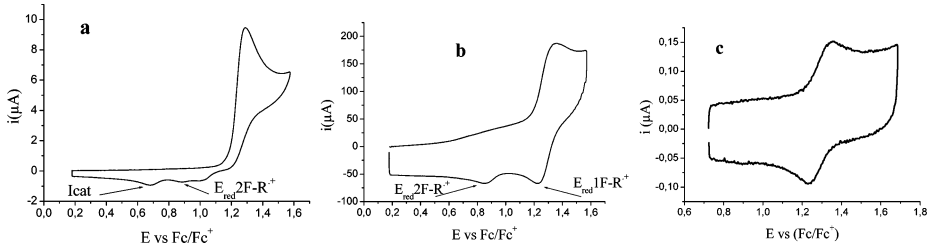

Figure 2. Cyclic voltammetry in CH_2Cl_2 (+0.2 mol·L^{-1} Bu_4NPF_6) of the oxidation of 1F−C_3H_7 (10^{-3} mol·L^{-1}) on a 1 mm diameter platinum disk electrode (scan rates (a) 0.2 and (b) 200 V·s^{-1}) and of the oxidation of 1F−C_2H_5 (10^{-3} mol·L^{-1}) on a 10 μm diameter platinum disk electrode (scan rate (c) 3800 V·s^{-1}).

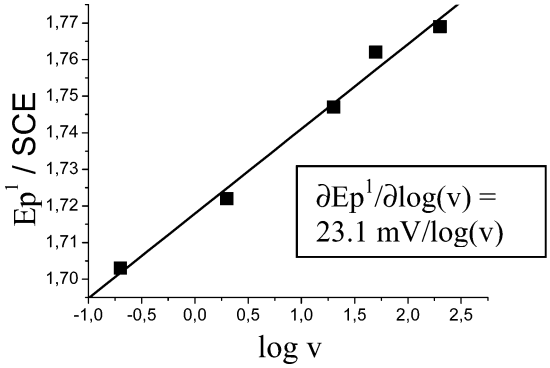

Figure 3. Variation of the oxidation peak potential E_p^1 with log(υ). The slope $\partial E_p^1/\partial[\log(\upsilon)] = 23.1$ mV/log(υ). E_p^1 values at different scan rates were measured during cyclic voltammetry recorded during the oxidation of 1F−C_3H_7 (concentration 10^{-3} mol·L^{-1}) in CH_2Cl_2 + Bu_4NPF_6 (0.2 mol·L^{-1}) on a 1 mm diameter platinum disk electrode.

can be ascribed to the monoelectronic reversible electron transfer of the dimer 2F−$R^{\bullet+}$/2F−R and thus shows that 2F−R is produced during the oxidation of the fluorene (the second oxidation of the dimer 2F−$R^{\bullet+}$/2F−R^{2+} and the oxidation of 1F−R are located at the same potentials).

The cathodic current corresponding to a peak located at ca. 0.0 V is associated in part with the reduction of a small amount of insoluble oligomers deposited on the electrode along the cycling, and in a second part with the proton reduction (these protons are released along the dimerization process[8]) since this current decreases when oxidation is performed on a vitreous carbon electrode instead of a platinum one. When the cycle is more positive than E_p* (Figure 1b), it is noticeable that the currents related to the product reduction are higher than the current related to the product oxidation at the following recurrent scan. The shape of the voltammograms suggests that the cathodic current is the sum of the contributions due to the undoping of a deposited polymer and to the reduction of the dimer and soluble oligomers.[15] These observations indicate that the oxidation of 1F−R leads to a mixture of dimer 2F−R, oligomers, and insoluble polymer. The faradic polymerization yield measured from the response of the deposited film in a blank solution versus the oxidation charge passed during the synthesis is around 15% in the experimental conditions of Figure 1. In the case of 1F−H, this value is very low when compared with the polymerization yield in acetonitrile, which is close to 100%.[16]

(15) Higher solubility of the reduced oligomers when compared to that of the oxidized oligomers would lead to a partial redissolution of the oligomers during the reverse scan and thus will also contribute to an increase in the dissymmetry between the oxidation and reduction peaks.

Table 1. Electrochemical Data in CH_3CN and CH_2Cl_2 for Monofluorenes 1F−R

monomer	solvent	$E°$ (V) vs Fc/Fc^+	$\partial E_p/\partial(\log(\upsilon)$ (mV/decade)	k_s (cm/s)	k_{dim} (L·mol^{-1}·s^{-1})
1F−H	CH_3CN	1.24	23	0.55	(2−3) × 10^8
1F−CH_3	CH_3CN	1.30	23	0.75	(0.8−1) × 10^8
1F−C_2H_5	CH_3CN	1.31	23.2	0.8	(5−6) × 10^7
1F−C_3H_7	CH_3CN	1.30	20.8	0.8	(3-4) × 10^7
1F−H	CH_2Cl_2	*a*	21.5	*a*	*a*
1F−CH_3	CH_2Cl_2	1.31		0.5	(0.8−1) × 10^7
1F−C_2H_5	CH_2Cl_2	1.29	22.4	0.8	2 × 10^6
1F−C_3H_7	CH_2Cl_2	1.29	23.2	0.5-0.6	(1−2) × 10^6

[a] Due to the difficulty in determining the $E°$ value of 1F−H in CH_2Cl_2, it was not possible to reach k_s and k_{dim} values for 1F−$H^{\bullet+}$ in CH_2Cl_2.

When the scan rates are increased to 200 V·s^{-1}, the currents of the products dimer (E_{red}(2F−$R^{\bullet+}$)), oligomers, and polymer (I_{cat}) decrease to the point of vanishing as the oxidation peak of the fluorene E_{red}(1F−$R^{\bullet+}$) becomes more and more reversible (see Figure 2a,b). Their total disappearance is observed for scan rates higher than 2000 V·s^{-1} as the 1F−$R^{\bullet+}$/1F−R system becomes fully reversible (Figure 2c), indicating that 1F−$R^{\bullet+}$ is stable during this experimental time (lifetimes around 50−100 μs).

For lower scan rates when the first oxidation is irreversible, the anodic peak potential E_p^1 is found to vary linearly with the scan rate υ (slopes close to 20 mV per 10-fold increase of υ in CH_2Cl_2; see Figure 3 and Table 1).

These slopes indicate that the rate-determining step is a second-order reaction in radical cation.[17] Moreover, the scan rate value required to observe the reversibility is dependent on the monomer concentration.[18] These observations are consistent with a rate-determining reaction involving the coupling of two radical cations formed upon fast electron transfer from monofluorenes (RC−RC coupling or DIM1 mechanism[17]):

$$1F-R \rightleftarrows 1F-R^{\bullet+} + e^- \; (E_{1F-R/1F-R^{\bullet+}}°, k_s)$$

$$1F-R^{\bullet+} + 1F-R^{\bullet+} \rightarrow 2F-R^{2+} \; (k_{dim})$$

The same experiments performed in acetonitrile (0.1 mol·L^{-1} Bu_4NPF_6) give similar slopes, indicating that the first steps

(16) Rault-Berthelot, J.; Angely, L.; Delaunay, J.; Simonet, J. *New J. Chem.* **1987**, *11*, 487.

(17) (a) Andrieux, C. P.; Savéant J.-M. In *Investigations of rates and mechanisms*; Bernasconi, C. F., Ed.; Wiley: New York, 1986; Vol. 6,4/E, Part 2, pp 305−390. (b) Bard, A. J.; Faulkner L. R. *Electrochemical methods. Fundamentals and applications*, 2nd ed.; John Wiley and Sons: New York, 2001.

(18) When the initial monomer concentration is increased, the reversibility appears for higher scan rates, meaning that the lifetime of the electrogenerated radical cation is lower.

of the mechanism are the same in both media even if the global polymerization yields may depend on the solvent due to its possible influence on the chemical steps following the first carbon−carbon bond formation.

Considering this mechanism, we measured the dimerization rate constants, k_{dim}, by comparing the experimental reversibility (for scan rates higher than 1000 $V \cdot s^{-1}$) with simulated curves (see the Experimental Section). Depending on the substituents R, the dimerization rate constants for $1F-R^{\bullet+}$ range from 3×10^7 to 10^8 $L \cdot mol^{-1} \cdot s^{-1}$ in CH_3CN and from 10^6 to 10^7 $L \cdot mol^{-1} \cdot s^{-1}$ in CH_2Cl_2. The higher reactivity of $1F-R^{\bullet+}$ in CH_3CN is related to the variation of the Coulombic repulsion during a coupling reaction that involves two charged species in solvents with different dielectric constants. However, in both solvents, k_{dim} values remain several orders below the diffusion-limited rate constant (2×10^{10} $L \cdot mol^{-1} \cdot s^{-1}$ in CH_3CN).[19] A small effect on k_{dim} from the nature of the substituent on the C_9 position is noticeable and can be related to a slight increase of the steric hindrance. From the reversible voltammograms, we can also extract the kinetic and thermodynamic values for the first electron transfer corresponding to the formation of the radical cations $1F-R^{\bullet+}$. The heterogeneous electron-transfer standard rate constants k_s (uncorrected from the double-layer effect) were estimated from the separation between the cathodic and anodic peak potentials.[17] We obtained values in the range $0.5-0.8$ $cm \cdot s^{-1}$, corresponding to a moderately fast electron transfer (Table 1) in agreement with the values expected for delocalized aromatic radical cations. The formal potentials E for $1F-R^{\bullet+}/1F-R$ couples were measured as the half-sum between peak potentials for the forward and the backward cycles (see Table 1). Obviously, substitution on the C_9 position does not significantly affect the E of the fluorenes. Due to the higher reactivity of $1F-H^{\bullet+}$, we were only able to measure the dimerization rate constant in CH_3CN; the high-scan-rate voltammograms were too distorted to be exploited in CH_2Cl_2. In that case, the derived value of k_{dim} is higher ($(2-3) \times 10^8$ $L \cdot mol^{-1} \cdot s^{-1}$) than for $1F-R^{\bullet+}$ (3×10^7 to 10^8 $L \cdot mol^{-1} \cdot s^{-1}$).

Polyfluorenes were also obtained in this medium by oxidation at a fixed potential when the electrode was maintained at a potential slightly more positive than that of the first peak (at $E_p^1 + 0.1$ V); however, the polymerization rate greatly increases when the electrode potential is fixed after the second process at $E_p^* \pm 0.1$ V.

Oxidation of 9,9-Disubstituted 2,7′-Difluorenes 2F−R. As observed in Figure 4a, oxidation of dimer 2F−R presents two well-defined reversible monoelectronic processes located at potentials E_p^1 (about 1.0 V) and E_p^2 (about 1.4 V) followed by a small irreversible peak located at E_p^* (about 1.6 V). These two first anodic processes correspond to the reversible formation of its dimers radical-cations $2F-R^{\bullet+}$ and dications $2F-R^{2+}$. The oxidation potentials for 2F−R are much lower than for the corresponding monomer, showing a higher stabilization of the produced radical cations and dications as expected from a larger charge delocalization. The third peak displays a smaller intensity than the first two peaks

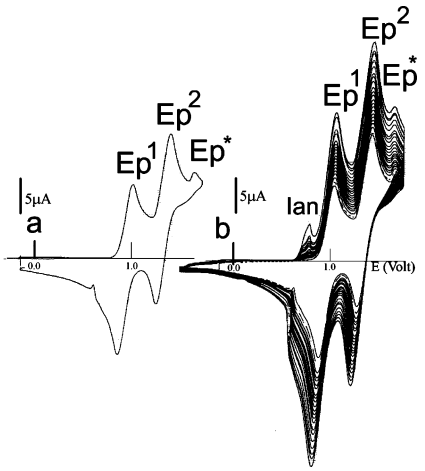

Figure 4. Cyclic voltammetry in dry $CH_2Cl_2 + 0.2$ $mol \cdot L^{-1}$ Bu_4NPF_6 in the presence of $2F-CH_3$ (10^{-2} $mol \cdot L^{-1}$) on a 1 mm platinum disk electrode: (a) one cycle, (b) multiple cycles between 0.0 and 1.83 V. Scan rate 0.1 $V \cdot s^{-1}$.

and appears at the same potential value E_p^* as that previously observed for the second process during 1F−R oxidation (vide supra). When the scan rate is increased, this peak disappears for scan rates higher than $1-2$ $V \cdot s^{-1}$, indicating that it corresponds to a species formed from a slow process during the oxidation of 2F−R. Cycling in a potential range including the first two reversible waves does not lead to any considerable modification of the electrochemical response, confirming that $2F-R^{\bullet+}$ and $2F-R^{2+}$ are stable species. On the contrary, large modifications are immediately detected when the reverse potential is rendered more positive than the E_p^* value. One can observe the appearance of a small anodic wave I_{an} (located before E_p^1) and the regular increase of the current (see Figure 4b). The electrode is covered by an insoluble and electroactive film deposited during the cycling. This evolution is however more pronounced in the case of $2F-CH_3$ than for the other 2F−R fluorenes, certainly because the longer alkyl chain on the C_9 position increases the solubility of the polymer (or oligomer) that diffuses in the solution instead of precipitating onto the electrode surface. We also observed that the polymerization yields of 2F−R are smaller than those of 1F−R, which may be due to the stability of the intermediate radical cation species, which present a higher tendency for diffusing in solution before the coupling reaction.

It is important to notice that polymers obtained during difluorene 2F−R oxidations display the same electrochemical behavior as those obtained by oxidation of monofluorenes 1F−R (see Figure 5), meaning that similar materials are electrogenerated in both cases. Except for poly(1F−H), which is not electroactive in the negative potential range, polymers derived from 1F−R and 2F−R have similar electrochemical responses (see Figure 5 for the example of poly($1F-C_2H_5$) and poly($2F-C_2H_5$)). The polymer p-doping and n-doping processes occur between 0.0 and 1.0 V and between −2.0 and −2.8 V, respectively. As already described, poly(1F−H) does not exhibit any n-doping process[16] due to the presence of two hydrogen atoms on the C_9 positions. Reduction to very negative potentials leads to a decomposition of the polymer (reduction in fluorenyl radical anion and generation of fluorenyl anion with hydrogen

(19) Andrieux, C. P.; Blocman, C.; Dumas-Bouchiat, J. M.; M'Halla, F.; Savéant, J.-M. *J. Am. Chem. Soc.* **1980**, *102*, 3806.

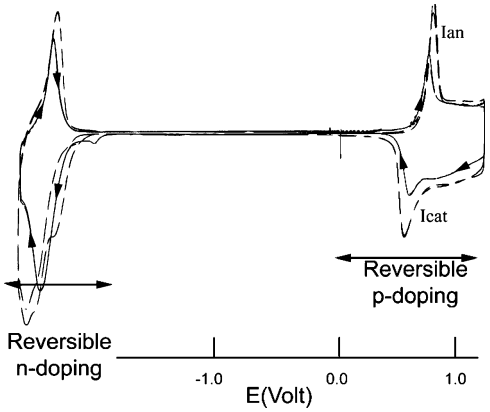

Figure 5. Comparative cyclic voltammetry in CH_3CN + 0.1 M Bu_4NPF_6 of electrogenerated films of poly($F-C_2H_5$) on a 1 mm platinum disk electrode. The polymers were previously deposited from the oxidation of $1F-C_2H_5$ (straight line and arrows) and $2F-C_2H_5$ (dashed lines). Scan rate 0.1 $V\cdot s^{-1}$.

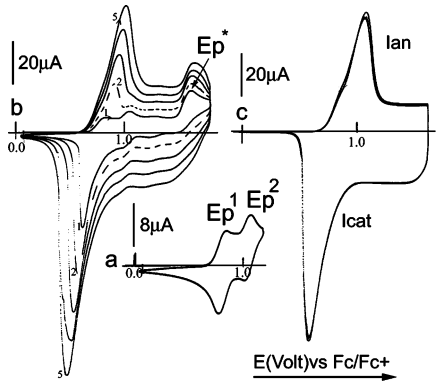

Figure 6. Cyclic voltammetry in dry CH_2Cl_2 + 0.2 $mol\cdot L^{-1}$ Bu_4NPF_6 (scan rate 0.1 $V\cdot s^{-1}$) (a, b) in the presence of $3F-C_3H_7$ (5×10^{-3} $mol\cdot L^{-1}$) on a 1 mm platinum disk electrode: (a) multiple cycles between 0.0 and 1.2 V, (b) multiple cycles between 0.0 and 1.83 V. (c) Anodic behavior of the poly($3F-C_3H_7$) synthesized in (b) and studied in the absence of $3F-C_3H_7$ in CH_2Cl_2.

evolution from carbon 9 of the fluorene unit). This electrochemical process leads to an irreversible destruction of the poly(*n*F−H).

Oxidation of the 9,9-Dipropyl-2,7′;2′,7″-terfluorenes, $3F-C_3H_7$. Due to solubility limitation, $3F-C_3H_7$ was the only trimer that we prepared. Its oxidation involved two well-defined reversible electron transfers, E_p^1 (0.86 V) and E_p^2 (1.08 V) (Figure 6a). The first oxidation that can be ascribed to the formation of the radical cation $3F-C_3H_7^{\bullet+}$ occurs at a lower oxidation potential than those required for $1F-C_3H_7^{\bullet+}$ and $2F-C_3H_7^{\bullet+}$. Simultaneously, the potential difference between the first and the second formal potentials $E_1°$ and $E_2°$ is only 220 mV for $3F-C_3H_7$, which is less than the corresponding value measured for $2F-C_3H_7$ (around 400 mV). The decreases of $E_1°$ and of the difference $E_2° - E_1°$ fall in line with the behavior observed when the length of π-conjugated molecules is increased, in carotenoids[20a] or other thiophene-based systems.[20b] It shows that, at least for the first three members of the oligofluorene series, the conjugation continuously increases with the chain length.

Table 2. Electronic Properties of Mono-, Di-, Ter-, and Polyfluorenes[a]

	λ_{max} (nm)	E_p^1 (V)		λ_{max} (nm)	E_p^1 (V)
1F−H and 1F−R	265	1.3	poly(1F−H)	355	
2F−R	327	1.0	poly(1F−R)	380	
$3F-C_3H_7$	353	0.86			

[a] Absorption spectra were recorded in CH_2Cl_2 solutions for the oligomers and as thin deposits on ITO electrodes for the polymers.

The two reversible processes are followed by another irreversible oxidation (located at a much more positive potential, $E_p^* \approx 1.6$ V). Recurrent cycles in a potential range including the first two reversible waves (Figure 6a) do not lead to film formation, which only occurs when the inversion potential reaches the threshold oxidation potential of E_p^*. Figure 6b shows five recurrent cycles recorded during $3F-C_3H_7$ oxidation, and the film formation is indicated by a regular increase of the intensity after each cycle.

The deposited film examined in a solution free of $3F-C_3H_7$ (Figure 6c) presents a reversible redox system with a threshold oxidation potential that is only slightly more positive (70 mV) than the oxidation potential of the trimer and in which the range of stability is very large (up to 1.7 V). When compared with that of poly($1F-C_3H_7$), the p-doping process of poly($3F-C_3H_7$) has a threshold oxidation potential shifted 0.1 V toward more positive potentials, showing that poly($3F-C_3H_7$) may be constituted of shorter oligomers. Moreover, the thin shape of the poly($3F-C_3H_7$) p-doping CVs and the symmetry between the anodic and cathodic currents suggest the main formation of one oligomer with a defined length (certainly the first coupling product, i.e., the oligomer containing six fluorene units) rather than the formation of a polymer or distribution of oligomers leading to a broader response which occurs in poly($1F-C_3H_7$). The oligomerization yield of $3F-C_3H_7$ is higher than 80% in those conditions.

UV−Vis Absorption of 1F−H, 1F−R, 2F−R, $3F-C_3H_7$ and the Derived Polymers Poly(1F−H) and Poly(1F−R). UV−vis absorption spectra of monofluorenes 1F−H and 1F−R, difluorenes 2F−R, and terfluorene $3F-C_3H_7$ were recorded in CH_2Cl_2 solutions. The λ_{max} values of the different compounds are gathered in Table 2. Whatever the nature of the alkyl group, all fluorenes and difluorenes display similar absorption spectra, with λ_{max} values of about 265 and 327 nm, respectively. The regular red shift goes on with $3F-C_3H_7$ (λ_{max} = 353 nm) and shows a continuous extension of the conjugation length upon oligomerization as described for well-defined oligomers (see, for example, ref 20b and references therein) and in accordance with the shift of their E_p^1 oxidation values.

All poly(1F−R) polymers electrogenerated on semitransparent ITO glasses present similar spectra with a λ_{max} around 380 nm, corresponding to a red shift of 30 nm in comparison with poly(1F−H) and in accordance with λ_{max} values of polyfluorenes and copolyfluorenes.[21]

(20) (a) Hapiot, P.; Kispert, L. D.; Konovalov, V. V.; Savéant, J.-M. *J. Am. Chem. Soc.* **2001**, *123*, 6669. (b) Frère, P.; Raimundo, J.-M.; Blanchard, P.; Delaunay, J.; Richomme, P.; Sauvajol, J.-L.; Orduna, J.; Grarin, J.; Roncali. J. *J. Org. Chem.* **2003**, *68*, 7254.

(21) Kreyenschmidt, M.; Klaerner, G.; Fuhrer, T.; Ashenhurst, J.; Karg, S.; Chen, W. D.; Lee, V. Y.; Scott, J. C.; Miller, R. D. *Macromolecules* **1998**, *31*, 1099.

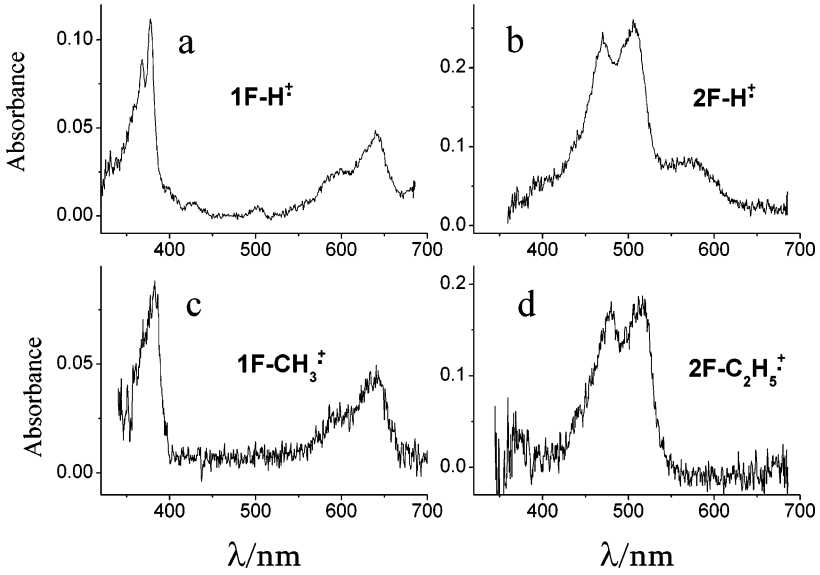

Figure 7. Differential UV−vis absorption spectra of the radical cations measured 300 ns after the laser pulse by irradiation of a solution of (a) 1F−H (1.1×10^{-5} mol·L^{-1}), (b) 1F−CH_3 (8.6×10^{-5} mol·L^{-1}), (c) 2F−H (7.8×10^{-5} mol·L^{-1}), and (d) 2F−C_2H_5 (4.5×10^{-5} mol·L^{-1}) in CH_3CN + CCl_4 (1%).

UV−Vis Absorption of Electrogenerated Radical Cations. Laser flash photolysis was used to record the UV−vis spectra of the radical cations. The same technique has been used successfully to characterize other oligomer radical cations in the thiophene or in the pyrrole series.[7d] Acetonitrile solutions of fluorene derivatives in the range 10^{-4} to 5×10^{-5} mol·L^{-1} were irradiated with short pulses of an excimer laser ($\lambda = 308$ nm) in the presence of 1% CCl_4, acting as an irreversible electron scavenger and allowing a fast production of the radical cation nF−R$^{\bullet+}$:

$$n\text{F}-\text{R} \xrightarrow{\text{CCl}_4,\, h\nu} n\text{F}-\text{R}^{\bullet+} + \text{CCl}_3^{\bullet} + \text{Cl}^-$$

Differential absorption spectra of fluorene, 9,9-dialkylfluorenes, 9,9-dialkyldifluorenes and their corresponding radical cations were recorded immediately (300 ns) after the laser pulse irradiation to limit the occurrence of possible chemical transformations (Figure 7). Fluorene radical cation 1F−H$^{\bullet+}$ displays two absorption peaks: a very intense peak in the 380 nm range and a broader weaker absorption in the 590−660 nm range. Spectra of fluorene 1F−H$^{\bullet+}$ (in agreement with literature results)[22] are identical to those of the dialkylfluorenes 1F−R$^{\bullet+}$ and confirm that the substitution on C_9 does not considerably influence the fluorene backbone of the molecule (Figure 7a,b). Similar experiments were also performed with the corresponding dimers 2F−H$^{\bullet+}$ and 2F−R$^{\bullet+}$ (Figure 7c,d). The spectra display two main absorption peaks: 465 and 500 nm for 2F−H$^{\bullet+}$ and 480 and 510 nm for 2F−$C_2H_5^{\bullet+}$. As observed for monofluorene radical cations, spectra for the dialkylated 2F−R$^{\bullet+}$ are similar to those recorded for unsubstituted 2F−H$^{\bullet+}$. Due to its higher stability, the UV−vis spectrum of 3F−$C_3H_7^{\bullet+}$ was recorded in CH_2Cl_2 using classical spectroscopic measurements. It diplays an intense absorption peak in the 400−650 nm range with a maximum at 545 nm. The large red shift for the main absorption between 1F−R$^{\bullet+}$ and 2F−R$^{\bullet+}$ is indicative of a large delocalization of the unpaired electron on the whole dimer (see, for example, π-conjugated systems in ref 20b).[23] This result is also in agreement with the observed variation on the redox potentials (see the previous discussion).[20]

Polymerization Mechanism of Fluorene Derivatives. Several conclusions can be drawn from the previous results.

(i) Starting from the monomer, the initial coupling step leads to the formation of a dimer through the reaction between two radical cations according to Scheme 3. This initial dimerization in the electropolymerization process is exactly the same as that found for the electropolymerization of other conducting polymers (polypyrrole, polythiophene, ...).[6b,c,7] The formation of the C−C bond leads to a new dihydrodimer dication that will lose two protons to form the final dimer 2F−R (second reaction in Scheme 3, first line).[6−8] This step, which involves a C−H$^+$ acid, is generally slow[9] and depends on the solvent and basic impurities.[8] In the classical electropolymerization scheme (pyrrole, thiophene, ...), the electrogenerated dimer is easier to oxidize than the starting monomer, and gives a new dimer radical cation at the level of the monomer oxidation potential. Then this dimer radical cation will repeat the coupling step to form a tetramer, ...[6,24] For fluorene, if the initial step is clearly the same, the rest of this classical scheme does not seem valid. We observed that the polymerization does not occur if the

(22) (a) McClelland, R. A.; Mathivanan, N.; Steenken, S. *J. Am. Chem. Soc.* **1990**, *112*, 4857. (b) O'Neill, M. A.; Cozens, F. L.; Schepp, N. P. *Tetrahedron* **2000**, *56*, 6969. (c) Delcourt, M. O.; Rossi, M. J. *J. Phys. Chem.* **1982**, *86*, 3233.

(23) It is likely that another band at higher wavelength is probably present in the dimer 2F−H and 2F−R radical cation spectra as it is for the monomer radical cations, but it cannot be seen because of the limited available wavelength range in our flash photolysis UV−vis detection. The same remark may be made for the 3F−C_3H_7 radical cation spectrum.

(24) (a) It has been predicted through quantum chemical modeling concerning a different type of monomer (pyrrole) that, for the formation of a long oligomer, the mechanism might involve the coupling of the oligomer dication with a nonoxidized monomer unit instead of coupling of the two radical cations. If a similar change of mechanism is also possible during fluorene electropolymerization, it is very difficult to obtain kinetics information about this following reaction step. Moreover, the oligomer length required to pass from one mechanism to the other one should also be different in pyrrole and fluorene series. (b) Lacroix, J.-C.; Valente, R.-J.; Maurel, F.; Lacaze, P. C. *Chem.−Eur. J.* **1998**, *4*, 1667.

Scheme 3. First Steps of the Coupling Process of 1F−R and 2F−R

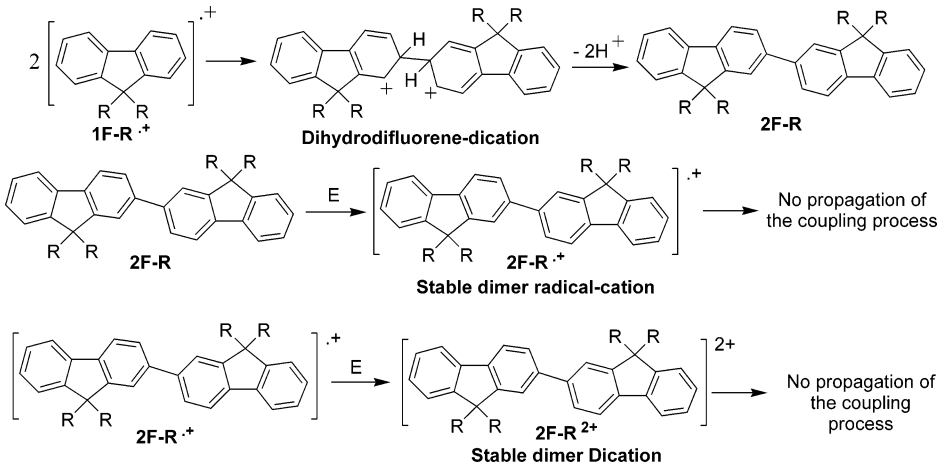

potential is maintained at the level of the formation of the dimer radical cation (Scheme 3, line 2).

(ii) Similarly, when starting from the dimers 2F−R, the oxidation leads to the formation of its radical cation and dication, but no polymerization occurs at this stage (Scheme 3, lines 2 and 3). One must oxidize to a third anodic E_p* wave level to trigger the polymerization.

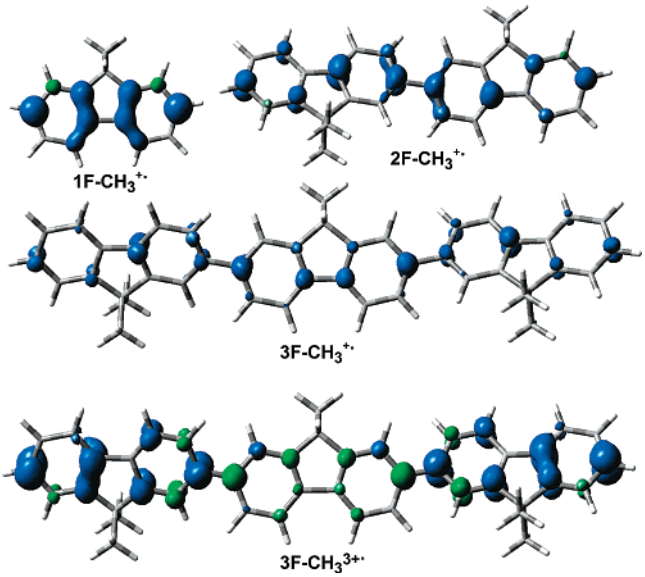

Figure 8. B3LYP/6-31G*-optimized structures and calculated spin densities (isodensity curves 0.004 ua) for 1F−$CH_3^{\bullet+}$, 2F−$CH_3^{\bullet+}$, 3F−$CH_3^{\bullet+}$, and 3F−$CH_3^{3\bullet+}$.

(iii) Starting from the trimer, the oxidation produces the radical cation, the dication, and certainly the radical trication, which leads to the film formation only at a high potential. To help in the interpretation of these puzzling observations, it is interesting to obtain information about the structure of the possible reactive intermediates.

Density functional theory calculations were used in this purpose to obtain the structure of the molecule and estimate the spin repartition. In radical chemistry, the quantity of unpaired electron that can be estimated through the calculated spin value is characteristic of the radical cation reactivity and selectivity.[25] Figure 8 shows the optimized conformations for the radical cations. Oligomer radical cations are not fully planar due to the steric hindrance between the fluorene rings (dihedral angles 24.0° and 27.9° in 2F−$CH_3^{\bullet+}$ and 3F−$CH_3^{\bullet+}$, respectively). Concerning the spin densities, the highest values are located on the external positions C_2 and C_7 (the Mulliken spin density on C_2 or C_7 is 0.284) in 1F−$CH_3^{\bullet+}$ and indicate that the coupling should principally occur on these carbon atoms as experimentally observed. For the dimer 2F−$CH_3^{\bullet+}$ and to a more extent in the trimer 3F−$CH_3^{\bullet+}$, although the spin density is present on all the fluorene rings, it is considerably decreased on the external carbons (Mulliken spin densities on the external carbons are 0.128 for 2F−$CH_3^{\bullet+}$ and 0.071 for 3F−$CH_3^{\bullet+}$)[25] and is more concentrated on the center of the molecule.

As previously noticed, the prediction of a spreading of the unpaired electron over the molecule is experimentally supported by the variation of electrochemical potentials and the red shift recorded on the UV−vis spectra (for the neutral and radical cation oligofluorenes), which indicate a regular increase of the conjugation with the chain length.[20] However, this dilution of the unpaired electron also predicts that the reactivity of the radical cation will rapidly decrease with the chain length. This means that the dimer radical cation is produced but is not reactive enough to couple and the polymerization stops at this level. To obtain the next coupling step, a more reactive intermediate has to be generated that can be achieved through the use of a more positive potential. A similar experimental situation has been described during the polymerization of di(benzylidene)tetrathiapentalenes into linear extented TTF polymer.[26] Similarly on a theoretical basis, the dilution of the unpaired electron has also been discussed for oligopyrrole series and has led the authors to suggest that further oxidation of the forming chains is needed for polymer growth, which is experimentally observed in our case.[24b] The following question is about the nature of this intermediate. In the case of 3F−$C_3H_7^{\bullet+}$, the characteristics of the voltammograms (Figure 6b) suggest that this intermediate is the trimer trication radical 3F−$C_3H_7^{3\bullet+}$, which is produced at a much more positive potential than those of the radical cation and dication. Calculations of the spin

(25) DFT geometry optimization tends to metalized organic radical cations; if this effect impacts the terminal carbon spin density, this known defect of DFT calculations will not modify the calculated trend.

(26) Hapiot, P.; Salhi, F.; Divisia-Blohorn, B.; Müller, H. *J. Phys. Chem. A* **1999**, *103*, 11221.

Scheme 4. Outcome of 2F−R$^{\bullet+}$ at E_p*

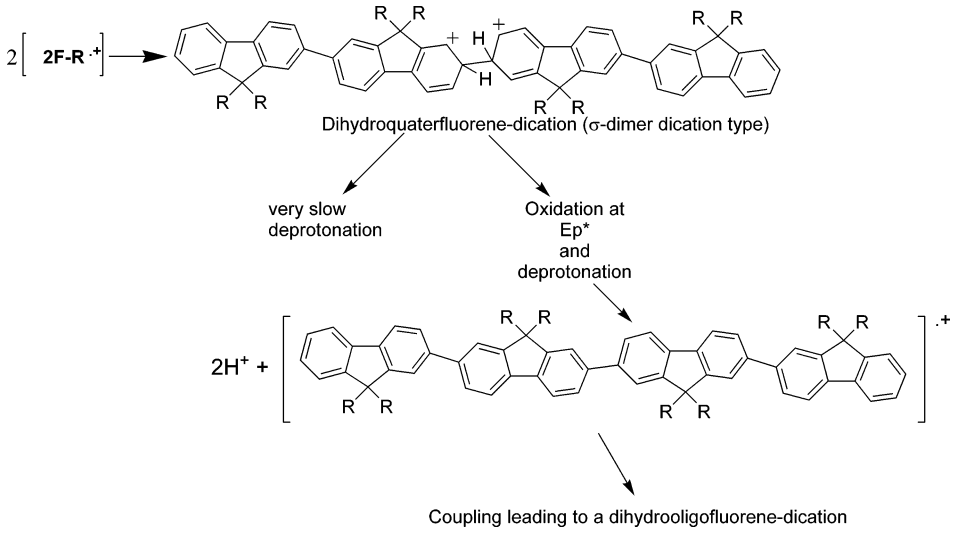

densities in 3F−$CH_3$$^{3\bullet+}$ show a very different distribution of the unpaired electron that is now pushed onto the external carbons and is thus expected to present a much higher reactivity for the coupling reaction (the Mulliken spin density is 0.23 on the external carbons). Even if the spin contamination is higher in the calculation of the trimer trication radical than for the dimer and monomer radical cations, the large difference appears significant of a much higher radical reactivity on the external carbon. If basically the conditions for polymerization appear similar for 1F−CH_3 and 2F−CH_3 taking into account the characteristics of current response associated with E_p*, the nature of the intermediates seems different but is essential to obtain the polymerization. Indeed, the height of the third oxidation peak current is dependent on the scan rate and initial fluorene concentration and remains small regarding the other electron transfers. These results suggest that the intermediate involved at this third stage comes from an evolution of the dimer radical cation or dication. All these observations are reminiscent of the behavior reported for stabilized oligomers that are not reactive enough for polymerizing but lead to "σ-dimer" carbocations (generally called "σ-dimers" in the literature).[27] With our compounds, these key intermediates may correspond to the dihydroquaterfluorene dication that is obtained, along a slow process, just after the carbon−carbon bond formation between 2F−R$^{\bullet+}$ (see Scheme 4).

Within the thiophene series, kinetic studies of the coupling steps between oligomers show that the stability of the intermediate σ-dimers (versus the deprotonation) increases as a function of chain length owing to a higher basicity of the dimers. This stability results in an increase of the reversibility degree of the coupling reaction that can lead to a manifold of electrochemical behaviors depending on both thermodynamic equilibrium and kinetic constants of the reaction (reversible dimerization).[28] This phenomenon has been observed for numerous radical coupling reactions and seems to be a general feature. In the field of conducting polymers, several examples have been reported for the radicals of oligoene oligomers,[27a] thianthrene[29] or substituted bithiophenes,[27b,e] and oligopyrroles[30] that reversibly dimerize, forming σ-dimer cations. It is likely that such a reversible σ-dimerization occurs during the electropolymerization of oligofluorenes such as 2F−R$^{\bullet+}$ and that the reaction will be less and less in favor of the coupling product formation when the number of fluorenes increases. Another electron transfer would partially displace the equilibrium and lead to the next oligomer (and then polymerization) after the elimination of two protons.

Conclusions

Electroactive polyfluorene films are obtained by anodic coupling of fluorene or 9,9-disubstituted fluorenes. The electropolymerization starts with the formation of the carbon−carbon bond through the coupling between two radical cations of fluorenes. This first step is very similar to the known mechanism demonstrated for other conducting polymers such as polypyrrole or polythiophene. However, the radical cation of the electrogenerated dimer is not reactive enough to repeat the coupling step as in the classical electropolymerization mechanism. This behavior is supported by DFT calculations that show a strong decrease of the unpaired electron density on the reactive positions (external carbons). To continue the polymerization, intermediates corresponding to higher oxidation states must be produced and the formation of polymers onto the electrode requires the use of more positive potentials (E_p*). For the longest oligomer 3F−C_3H_7, the intermediate has all the electrochemical characteristics

(27) (a) Smie, A.; Heinze, J. *Angew. Chem., Int. Ed. Engl.* **1997**, *36*, 363. (b) Tsuncky, P.; Smie, A.; Engelmann, G.; Kossmehl, G. *J. Electroanal. Chem.* **1997**, *433*, 223. (c) Heinze, J.; Tsuncky, P.; Smie, A. *J. Solid State Electrochem.* **1998**, *2*, 102. (d) Hübler, P.; Heinze, J. *Ber. Bunsen-Ges. Phys. Chem.* **1998**, *102*, 1506. (e) Heinze, J.; John, H.; Dietrich, M.; Tschuncky, P. *Synth. Met.* **2001**, *119*, 49.

(28) (a) Amatore, C.; Garreau, D.; Hammi, M.; Pinson, J.; Savéant, J.-M. *J. Electroanal. Chem.* **1985**, *1841*, 1. (b) El-Desoky, H.; Heinze, J.; Ghoneim, M. M. *Electrochem. Commun.* **2001**, *3*, 697.

(29) Hübler, P.; Heinze, J. *Ber. Bunsen-Ges. Phys. Chem.* **1998**, *102*, 1506.

(30) (a) Andrieux, C. P.; Hapiot, P.; Audebert, P.; Guyard, L.; An, M. Nguyen Dinh; Groenendaal, L.; Meijer, E. W. *Chem. Mater.* **1997**, *9*, 723. (b) Audebert, P.; Guyard, L.; Nguyen Dinh An, M.; Hapiot, P.; Chahma, M.; Combelas, C.; Thiebault, A. *J. Electroanal. Chem.* **1996**, *407*, 169.

of the trication radical, which exhibits a large spin density on the external reactive carbon (according to DFT calculations). It is noticeable that, in such a case, the oxidation leads to the formation of defined length oligomers. In the case of the fluorene or 2,7′-dimer oxidations, the polymeric films are produced. However, the nature of the high oxidation state intermediate was not completely elucidated. By analogy with literature results concerning the oxidations of conjugated oligomers (oligothiophenes, oligopyrroles, ...), the dimer radical cation should be in equilibrium with its corresponding σ-dimer dication, the dihydroquaterfluorene dication (this equilibrium can be thermodynamically unfavored). A new electron transfer may displace the equilibrium and allows the occurrence of the irreversible coupling.

CM048331O